Am J Transl Res 2024;16(4):1337-1352
www.ajtr.org /ISSN:1943-8141/AJTR0154154

Original Article

Comparative metabolomics of MCF-7 and MCF-7/TAMR identifies potential metabolic pathways in tamoxifen resistant breast cancer cells

Alok Mishra[1], Anubhav Srivastava[2], Anshuman Srivastava[1], Lokendra Kumar Sharma[2], Anand Kumar Mishra[3], Ashutosh Shrivastava[1]

[1]Center for Advance Research, Faculty of Medicine, King George's Medical University, Lucknow, Uttar Pradesh 226003, India; [2]Department of Molecular Medicine and Biotechnology, Sanjay Gandhi Postgraduate Institute of Medical Sciences, Lucknow, Uttar Pradesh 226014, India; [3]Department of Endocrine Surgery, Faculty of Medicine, King George's Medical University, Lucknow, Uttar Pradesh 226003, India

Received October 30, 2023; Accepted April 8, 2024; Epub April 15, 2024; Published April 30, 2024

Abstract: Objectives: Breast cancer is the most common cancer and the leading cause of cancer-related death among women. An Estrogen Receptor (ER) antagonist called tamoxifen is used as an adjuvant therapy for ER-positive breast cancers. Approximately 40% of patients develop tamoxifen resistance (TAMR) while receiving treatment. Cancer cells can rewire their metabolism to develop resistant phenotypes, and their metabolic state determines how receptive they are to chemotherapy. Methods: Metabolite extraction from human MCF-7 and MCF-7/TAMR cells was done using the methanol-methanol-water extraction method. After treating the dried samples with methoxamine hydrochloride in pyridine, the samples were derivatized with 2,2,2-Trifluoro-N-methyl-N-(trimethylsilyl)-acetamide, and Chlorotrimethylsilane (MSTFA + 1% TMCS). The Gas chromatography/mass spectrometry (GC-MS) raw data were processed using MSdial and Metaboanalyst for analysis. Results: Univariate analysis revealed that 35 metabolites were elevated in TAMR cells whereas 25 metabolites were downregulated. N-acetyl-D-glucosamine, lysine, uracil, tyrosine, alanine, and o-phosphoserine were upregulated in TAMR cells, while hydroxyproline, glutamine, N-acetyl-L-aspartic acid, threonic acid, pyroglutamic acid, glutamine, o-phosphoethanolamine, oxoglutaric acid, and myo-inositol were found to be downregulated. Multivariate analysis revealed a distinct separation between the two cell lines, as evidenced by their metabolite levels. The enriched pathways of deregulated metabolites included valine, leucine, and isoleucine degradation, Citric Acid Cycle, Warburg effect, Malate-Aspartate shuttle, glucose-alanine cycle, propanoate metabolism, and Phospholipid biosynthesis. Conclusion: This study revealed dysregulation of various metabolic processes in TAMR cells, which may be crucial in elucidating the molecular basis of the mechanisms underlying acquired tamoxifen resistance.

Keywords: Breast cancer, estrogen receptor, tamoxifen, drug resistance, metabolomics

Introduction

Breast cancer is one of the most prevalent cancers across the globe. In 2020, breast cancer affected 2.3 million women, resulting in a total of 685,00 deaths worldwide [1]. The development of accurate biomarkers for early detection, routine screening, and breast cancer prevention has helped to increase the survival rate of breast cancer patients. Moreover, the survival rate of patients also increased due to the introduction of novel chemotherapeutic approaches such as anti-HER2 therapy, anti-ER therapy, anti-PI3K, anti-mTOR therapy, and anti-PD1 immunotherapy [2]. Approximately 70-75% of invasive breast carcinomas have high estrogen receptor (ER) expression [3]. Tamoxifen (TAM), a nonsteroidal anti-estrogen drug, is most widely used to treat estrogen receptor-positive breast cancer. Dr. Arthur L. Walpole, during his tenure being in-charge of the ICI Pharmaceuticals Division's fertility control program, made the discovery of TAM [4]. Tamoxifen increases the overall survival when used as adjuvant therapy for early breast cancer, and is believed that its widespread usage

https://doi.org/10.62347/MJLN5908

has significantly contributed to the drop in breast cancer mortality [5].

Despite the clear advantages of tamoxifen in these therapeutic contexts, nearly all patients with metastatic disease and up to 40% of those taking adjuvant tamoxifen eventually experience relapse and succumb due to the acquired resistance to tamoxifen [6]. Loss of ER expression could result in resistance to therapy because tamoxifen's effects are predominantly mediated through the ER, and the level of ER expression is a good predictor of responses to tamoxifen. Although the majority of ER/PR-negative cancers do not respond to anti-estrogens, loss of ER expression is in fact the primary mechanism of *de novo* resistance to tamoxifen. Aromatase inhibitors or the ER-down-regulator fulvestrant can help up to 20% of patients who are not responding to tamoxifen. This shows that ER still controls growth in many of these TAMR cancers [7].

Several mechanisms have already been established for tamoxifen resistance, including the downregulation of the estrogen receptor alpha (ER), protective autophagy of drug-resistant cells, deregulation of cell cycle regulators, and the downregulation of transcription factors and enzymes that regulate estrogen receptor expression [8, 9]. Metabolic reprogramming is one of the hallmarks of cancer cells. Deregulated metabolism in cancer cells produces a significant quantity of metabolites, which are necessary for the production of macromolecules and may promote cancer growth, metastasis, and treatment resistance [10, 11].

Cancer cells can rewire their metabolism to develop resistant phenotypes, and their metabolic state determines how responsive they are to chemotherapy [12]. Cellular metabolomics is an important part of systems biology because it uses high-throughput detection technology to analyze intra- and extracellular small molecules (metabolites) qualitatively and quantitatively, which can be considered the best functional signature of phenotype, and to observe changes in metabolite concentration [13]. Mass spectrometry plays a significant role as a key analytical tool in the field of metabolomics. Mass spectrometry in combination with gas and liquid chromatography are the two most important analytical techniques for the study of metabolites in complex biological mixtures. Due to its much higher sensitivity and fast data acquisition, MS plays an increasingly important role in the field of metabolomics [14].

The effect of TAM and/or Paclitaxel treatment on the metabolomics of breast cancer cells MCF-7 and MDA-MB-31 was studied by utilizing GC-MS to identify key metabolites that are differentially abundant in TAM-treated cells, as well as pathways associated with these metabolites [15, 16]. A different study used another metabolomics approach based on proton nuclear magnetic resonance spectroscopy (1H-NMR) to study TAM resistance by comparing metabolites from MCF-7, MCF-7/TAMR, and choline kinase-α (CK-α) knockdown MCF-7/TAMR cells [17]. To date, no study has reported a GC-MS-based analysis of TAM resistant breast cancer cells. Human adenocarcinoma MCF-7 cells are estrogen and progesterone-receptor positive and represent the luminal A subtype [18]. The aim of this study was to compare the metabolic profiles of MCF-7 cells and MCF-7/TAMR cells using GC-MS-based metabolomics to unearth the differential metabolite levels and altered metabolic pathways that could pave the way for therapeutic targeting of drug-resistant breast cancer cells.

Materials and methods

Reagents

All reagents and chemicals used in this study were HPLC-grade. Water and methanol were purchased from Merck. 4-Hydroxytamoxifen was purchased from Sigma Aldrich (USA). Alkane standard mixture C_{10}-C_{40} (all even) was procured from Supelco. Ribitol (adonitol) and methoxyamine hydrochloride were purchased from Thermo Fisher (USA), pyridine from Thermo Fisher (USA), and N-Methyl-N-(trimethylsilyl) trifluoroacetamide with 1% trimethylchlorosilane (MSTFA + 1% TMCS) from SRL (Mumbai, India).

To establish MCF-7 and MCF-7/TAMR breast cancer cell culture

The MCF-7 human breast cancer cell line was procured from the National Repository for Cell

Lines, National Centre of Cell Sciences (Pune, India), and MCF-7/TAMR cells were purchased from American Type Culture Collection (ATCC). These cell lines were cultured in Dulbecco's Minimum Essential Medium (DMEM) containing 10% heat-inactivated Fetal Bovine Serum (FBS), 10 µg/mL insulin, 100 U/mL penicillin, and 100 µg/mL streptomycin at 37°C in a 95% humid atmosphere with 5% CO_2. MCF-7/TAMR cells were cultured in DMEM containing 1 µM 4-hydroxytamoxifen. Cells in a tissue culture flask (25 cm^2) were rinsed for maintenance with Ca^{++} and Mg^{++}-free PBS, pH 7.2, and the media was replaced every two days. Cells were divided using a trypsin solution when confluence reached 80-90%. In order to do this, the medium was aspirated, and cells were then rinsed with PBS for 1-2 minutes and then incubated for 1-2 minutes with 2 mL of a 0.5% trypsin solution containing EDTA-4 Na. After removing the trypsin solution, the flask was turned vertically for three to five minutes to cause cell separation. This was followed by the addition of fresh culture media, aspiration, and dispensing into brand-new culture flasks at a split ratio of 1:3-1:6.

Metabolite extraction

The samples were processed in triplicate. Two million cells were taken for metabolite extraction. The metabolites were extracted in three sequential steps. Initially, the cell pellets were resuspended in 500 µL cold MeOH (-20°C) and, 30 µl of ribitol solution (0.2 mg/ml in water) as an internal standard was added to each sample. After being vortexed for 30 seconds, the samples were quickly frozen in liquid nitrogen. The samples were centrifuged at 800 g for 1 minute at 4°C after being thawed at 37°C, and the supernatant was then transferred to a new centrifuge tube placed on dry ice. Once more, the freeze-thaw procedure was carried out with 500 µL of a cold MeOH solvent. Finally, 250 µL of ice-cold water was used for freeze-thaw extraction process, and the sample was centrifuged at 15,000 g for 1 min. The supernatant obtained from each extraction step (Methanol-Methanol-Water) was pooled together, and vacuum centrifugal evaporation was used to dry the samples, which were then kept at -80°C until analysis [19, 20]. Subsequently, the dried samples were mixed with 20 µL of MOX reagent, which contains 20 mg/mL of methoxyamine-hydrochloride in dry pyridine. A 90-minute incubation period in a digitally heated, shaking dry bath (Thermomixer, Eppendorf) at 30°C and 1100 rpm followed. The samples were derivatized by adding 80 µL of N-Methyl-N-(trimethylsilyl) trifluoroacetamide with 1% trimethylchlorosilane (MSTFA + 1% TMCS), followed by a 30-minute incubation in Thermomixer at 60°C.

GC-MS analysis

Chromatographic separation of derivatized samples was achieved by using a GC-MS outfitted with a Triplus 100 autosampler, a Trace 1300 gas chromatograph, and a TSQ 8000 (Thermo Fisher Scientific) Triple Quadrupole Mass Spectrometer. The Trace GOLD TG-5MS (Thermo Scientific) column, which has a diameter of 0.25 mm, a thickness of 0.25 mm, and a length of 30 m, was used for the analyte separation. The oven's temperature was raised from 50°C for one minute to 100°C at a rate of 6°C per minute, 200°C at a ramp rate of 4°C per minute, and then 280°C at a rate of 20°C and held for three minutes. The temperatures of the injection port, ion source, and transfer line were 250°C, 250°C, and 200°C, respectively. Helium was used as a carrier and argon as a collision gas. The metabolites were fragmented using electron ionization (EI) with an energy of 70 electron volts (eV). The analysis was conducted using the full scan mode, covering a mass range of 50 to 650 Daltons with a solvent delay of 4 minutes [21].

Data analysis

Preprocessing of GC-MS data: GC-MS generate raw data in '.raw' format. The raw data were converted to an abf file format and processed using MS-DIAL (mass spectrometry-data independent analysis) [22]. Further analysis was performed by selecting hard ionization (GC-MS) as the ionization type and data-dependent mode in MS-DIAL. Using default MS-DIAL settings, processed mass spectra were created, consisting of peak masses and their area intensities. The minimum peak width and height were 5 and 1000, the MS1 was centroid, the ion mode was positive, the mass range was 50-650 Dalton, the retention time range was

0-40.5 min, the mass tolerance was 0.25 m/z, the retention time tolerance was 5 s. The EI spectra cutoff was set to 10 amplitude, and the sigma window value was set to 0.5 for the MS1 deconvolution. Annotation was performed using the "All records with Kovats RI (9062 unique compounds)" EI-MS library available on the MSdial website, which contain data from Fiehn DB, RIKEN DB, Kazusa DB, and MoNA volatile, by comparing the processed mass spectra data against the libraries with an 80% identification score cut off [23]. Annotated metabolites were confirmed by using the National Institute of Standards and Technology (NIST) mass spectral library available in GC-MS system.

Metabolomics statistical analysis: Pre-processed metabolite data with related peak area was statistically analyzed using the web-based tool 'MetaboAnalyst 5.0' https://www.metaboanalyst.ca/ (retrieved on February 10, 2022) [24]. Interquartile range (IQR) statistical filter was selected while performing data filtering. To reduce systematic biases within the sample of the experiment, total area normalization was used [25]. To remove offsets and equalize the importance of high- and low-abundance metabolites, the data were log-transformed and Pareto scaled for multivariate analysis. PCA displayed the original data distribution. To achieve a high level of group separation and to identify the variables responsible for classification, supervised Orthogonal Partial Least Squares Discriminant Analysis (OPLS-DA) was used. Sevenfold cross-validation was used to validate the OPLSDA model. The model's quality was evaluated using R2 and Q2 scores, and the permutation test was used to validate it. To identify significantly differentially abundant metabolites between control and TAMR, the OPLS-DA model was used with the first principal component of Variable Importance in Projection (VIP) values and the Student's t-test. To correct for multiple comparisons, the q values (adjusted *P* values), which were raw *P* values from the t-test adjusted using the Benjamini and Hochberg procedure (BH method), were used. By comparing the mean values of the peak areas obtained from the control and TAMR, the fold change in metabolite abundance was calculated. Box and whisker plots were generated for downregulated and upregulated metabolites. The enrichment analysis was performed by using the metabolite concentration table in .csv format. It uses a generalized linear model to estimate a Q-statistic for each set of metabolites. This model shows how compound concentration profiles are related [26].

Results

Metabolite identification

The aim of this study was to use GC-MS to explore the metabolism of MCF-7 and MCF-7/TAMR cells in order to identify altered metabolic pathways during tamoxifen resistance in breast cancer. The full-scan GC-MS chromatograms of MCF-7 and MCF-7/TAMR cells are represented in **Figure 1**. Two experimental repeats were performed in order to observe patterns and trends in the results and ensure the integrity of the data. Pooled QC mixtures were analyzed to check system stability. The PCA plot (Supplementary Figure 1) effectively demonstrates the clustering patterns seen among quality control (QC) samples, which indicates the stability of the GC-MS platform was satisfactory throughout the experiment. A total dataset of 2025 features was generated. To facilitate the calculation of Kovats retention indices, an alkane standard mixture C_{10}-C_{40} (all even carbon) was analyzed using the same instrument parameters. Metabolite identification was performed based on MS spectra and retention indices (RI). The set of compounds that met the criteria and showed MS with RI was then annotated using the spectral library. A total of 114 compounds were selected for further statistical analysis.

Identification of deregulated metabolites in TAMR cells

To investigate the impact of TAM resistance on metabolite levels and to identify significant differences in metabolites between control MCF-7 and MCF-7/TAMR cells, we used a Student t-test and fold change analysis. There were a total of 60 significant metabolites discovered out of a total of 114 identified metabolites. The criteria for significance were a fold change (FC) threshold of 2 and a p-value ≤ 0.05. Out of a total of 60 metabolites, 35 were found to be upregulated in TAMR cells and 25 were found to be downregulated (**Table 1**). **Figure 2A** represents significant upregulated and downreg-

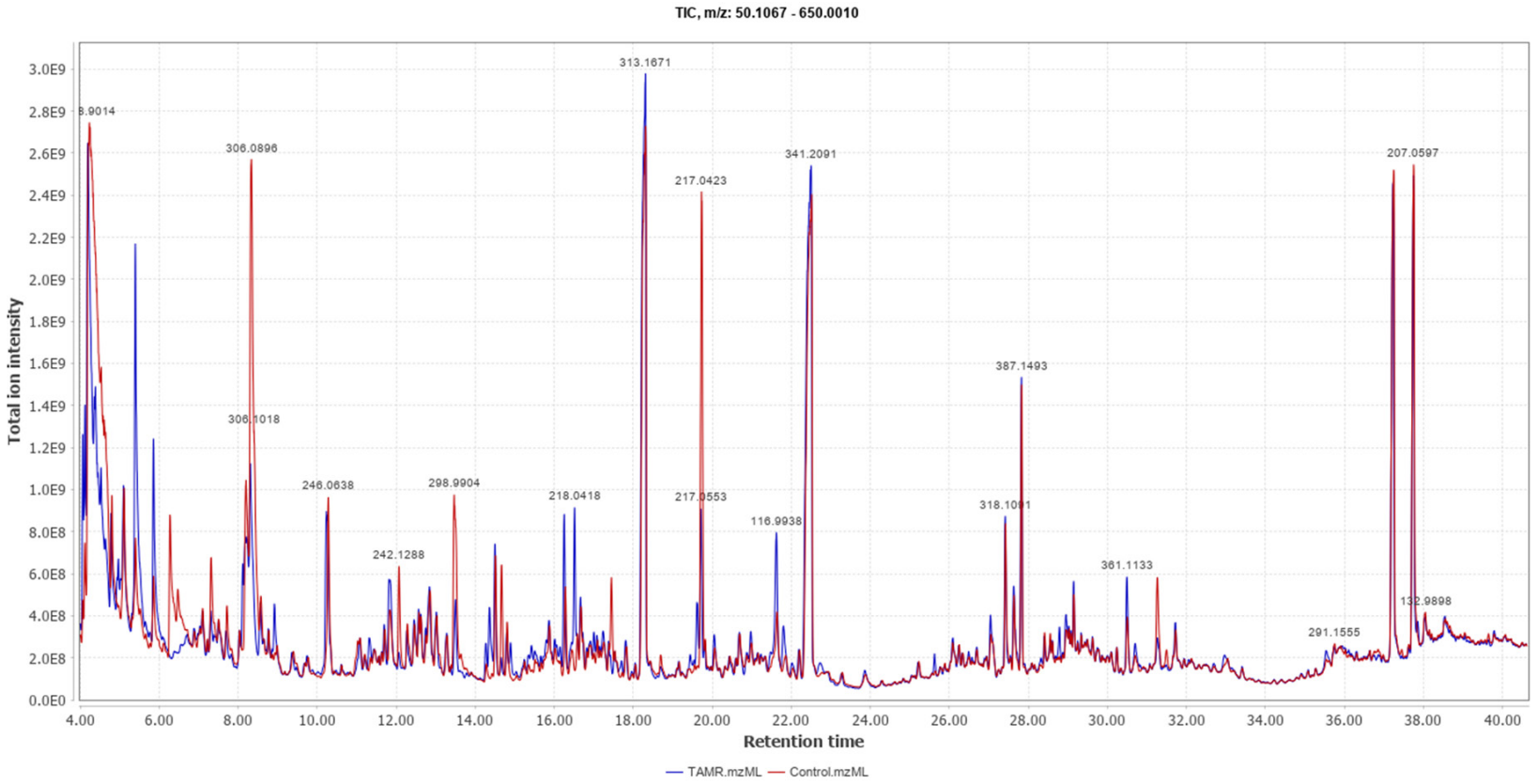

Figure 1. The overlay total ion chromatograms (TIC) by gas chromatography-mass spectrometry. The TIC from Control MCF-7 cells and MCF-7/TAMR cells are represented by the colors red and blue, respectively.

Table 1. Significant metabolite features obtained from volcano plot (fold change threshold of 2 and *p*-value ≤ 0.05)

Retention Time	Metabolites	Quant Mass	Fold Change	log2(FC)	raw.pval
19.62	N-Acetyl glucosamine	72.98	31.22	4.964	1.16E-10
20.73	Ribulose 5-phosphate	357.06	28.17	4.816	0.00013
16.25	L-Lysine	174.05	24.60	4.620	1.43E-5
11.86	Xylitol	217.06	17.29	4.111	4.32E-11
4.96	Uracil	241.05	11.00	3.459	2.08E-7
15.30	Pyridoxal	309.09	9.79	3.292	3.12E-11
14.12	Glycylglycine	174.06	9.11	3.188	7.55E-10
12.46	D-Arabitol	217.05	7.85	2.974	6.59E-9
14.36	Citrulline	157.07	7.77	2.958	0.00056
30.82	2-monostearin	129.02	7.30	2.869	7.13E-7
8.11	L-Methionine	176.04	6.56	2.715	1.93E-8
4.93	Glyceric acid	189.06	6.48	2.697	4.63E-5
16.51	Tyrosine	218.03	6.37	2.672	0.00122
11.86	D-Ribulose	205.07	5.73	2.520	8.96E-10
28.76	Docosahexaenoic acid	79.018	5.13	2.359	2.11E-5
21.81	Oleic acid	116.99	4.95	2.309	2.26E-5
21.80	Elaidic acid	117.00	4.92	2.299	2.29E-5
33.92	Galactinol	204.07	4.67	2.225	0.00190
15.43	Hydroxyphenyllactic acid	179.03	4.17	2.062	0.00231
13.841	Phosphoserine	299.099	4.09	2.030	2.2058E-4
16.05	Glucose	205.07	3.99	1.999	1.13E-8
6.55	L-Aspartic acid	160.05	3.92	1.972	1.36E-6
4.06	L-Isoleucine	158.09	3.78	1.918	8.80E-7
17.65	Pantothenate	291.07	3.74	1.906	1.23E-14
10.23	Phenylalanine	218.05	3.66	1.875	2.29E-6
17.01	Galactitol	217.05	3.32	1.733	2.52E-10
6.42	beta-Alanine	248.10	3.25	1.704	2.42E-6
5.39	L-Serine	204.07	3.05	1.613	4.67E-8
17.71	Trans-Hexa-dec-2-enoic acid	117.00	2.89	1.535	0.00019
25.63	Arachidonic acid	79.02	2.76	1.468	0.00463
5.51	beta-Cyano-L-Alanine	141.04	2.36	1.244	0.01385
31.32	Monooleoylglycerol	397.26	2.33	1.226	0.02405
4.38	L-Proline	142.04	2.22	1.156	3.88E-9
17.81	Palmitoleic acid	116.99	2.03	1.024	0.04308
5.85	DL-Allothreonine	218.08	2.02	1.015	2.70E-7
16.27	Galactose	319.09	0.45	-1.147	8.86E-11
8.18	DL-Pyroglutamic acid	156.02	0.44	-1.172	5.52E-09
10.27	L-Glutamic acid	246.07	0.44	-1.179	4.50E-11
11.54	L-Arabinose	217.06	0.43	-1.212	1.38E-05
4.53	Glycine	174.05	0.42	-1.218	0.002706
21.49	Linoleic acid	221.05	0.37	-1.423	2.85E-05
8.17	Gamma-aminobutyric acid	72.97	0.35	-1.504	2.05E-07
31.26	Lactitol	204.05	0.29	-1.756	0.00029
18.68	Inositol	217.05	0.28	-1.836	3.41E-11
14.50	Citric acid	273.03	0.25	-1.947	9.15E-05
7.44	DL-Malic acid	147.00	0.25	-1.949	8.86E-08

31.25	Lactose	204.03	0.25	-1.983	2.12E-07
8.98	Threonic acid	292.09	0.24	-2.053	8.90E-08
13.46	Glycerol 3-phosphoate	299.03	0.21	-2.199	4.74E-08
7.307	Aminomalonate	218.05	0.21	-2.212	1.51E-06
11.31	L-Asparagine	231.09	0.19	-2.368	1.82E-08
5.04	3-Aminopropionitrile	245.03	0.16	-2.570	1.42E-07
13.63	O-Phosphoethanolamine	299.01	0.09	-3.374	5.52E-05
13.51	Glycerol 1-phosphate	217.03	0.08	-3.577	1.57E-12
26.02	Glucose 6-phosphate	299.01	0.07	-3.783	2.17E-05
8.40	Hydroxyproline	230.08	0.06	-3.986	3.60E-05
9.39	a-Ketoglutaric acid	198.01	0.04	-4.332	2.19E-09
13.33	D-Glutamine	156.05	0.03	-4.762	0.00166
10.99	N-Acetyl aspartic acid	158.05	0.03	-5.042	0.00029
21.99	L-Tryptophan	202.05	0.003	-8.049	5.40E-06

ulated metabolites obtained by the volcano plot. In addition, heat map analysis was used to look at the metabolites in the MCF-7 and MCF-7/TAMR samples. In this analysis, the sample information is represented on the horizontal axis, while the variable information is on the vertical axis. The red color signifies an increase, while the green color signifies a decrease in the concentration of metabolites (**Figure 3**).

Box and whisker plots of some important deregulated metabolites are shown in **Figure 4**. Among the significantly altered metabolites, N-Acetyl-D-glucosamine (fold change = 40, $P < 0.001$) was found to be the most upregulated metabolite, while tryptophan (fold change = 0.003, $P < 0.001$) was found to be the most downregulated metabolite in TAMR cells.

Identification of major discriminatory metabolites

For multivariate statistical analysis, unsupervised principal component analysis (PCA) and supervised Orthogonal Partial Least Squares Discriminant Analysis (OPLSDA) were performed to evaluate the separation between MCF-7 cells and MCF-7/TAMR cells. **Figure 2B** shows a PCA plot that clearly separates the two groups, indicating a substantial difference between the control and TAMR cell lines in terms of metabolite levels. The supervised Orthogonal Partial Least Squares Discriminant Analysis (OPLS-DA) model was developed to identify the relationship between metabolite expression level and both groups represented in **Figure 5A**. The OPLSDA model provided significant discriminating metabolites between MCF-7 cells and MCF-7/TAMR cells. The explained variation (R^2) and prediction capability (Q^2) of a random permutation test (n = 2000) were 0.971 and 0.96, respectively. Metabolites having a VIP score greater than 1 were considered most relevant for discriminating power (**Figure 5B**). Among the most important metabolites found are pyridoxal, inositol, galactitol, xylitol, n-acetyl-d-glucosamine, pantothenate, pyroglutamic acid, L-glutamic acid, glycyl-glycine, galactose, and D-ribulose.

Metabolite set enrichment analysis

Quantitative enrichment analysis (QEA) was performed to obtain enriched pathways related to deregulated metabolites. All the annotated metabolites with their corresponding peak areas were analyzed using two reference databases, Kyoto Encyclopedia of Genes and Genomes (KEGG) [27] and the small molecule pathway database (SMPDB) [28]. Tamoxifen resistance had a significant impact on glucose/energy metabolism, specifically on metabolic pathways that differed significantly between the two cell lines, such as valine, leucine, and isoleucine degradation, citric acid cycle, Warburg effect, malate-aspartate shuttle, mitochondrial electron transport chain, glucose-alanine cycle, folate metabolism, propanoate metabolism, and phospholipid biosynthesis. Deregulated enriched pathways are depicted in **Figure 6**, and **Table 2** represents the top 25

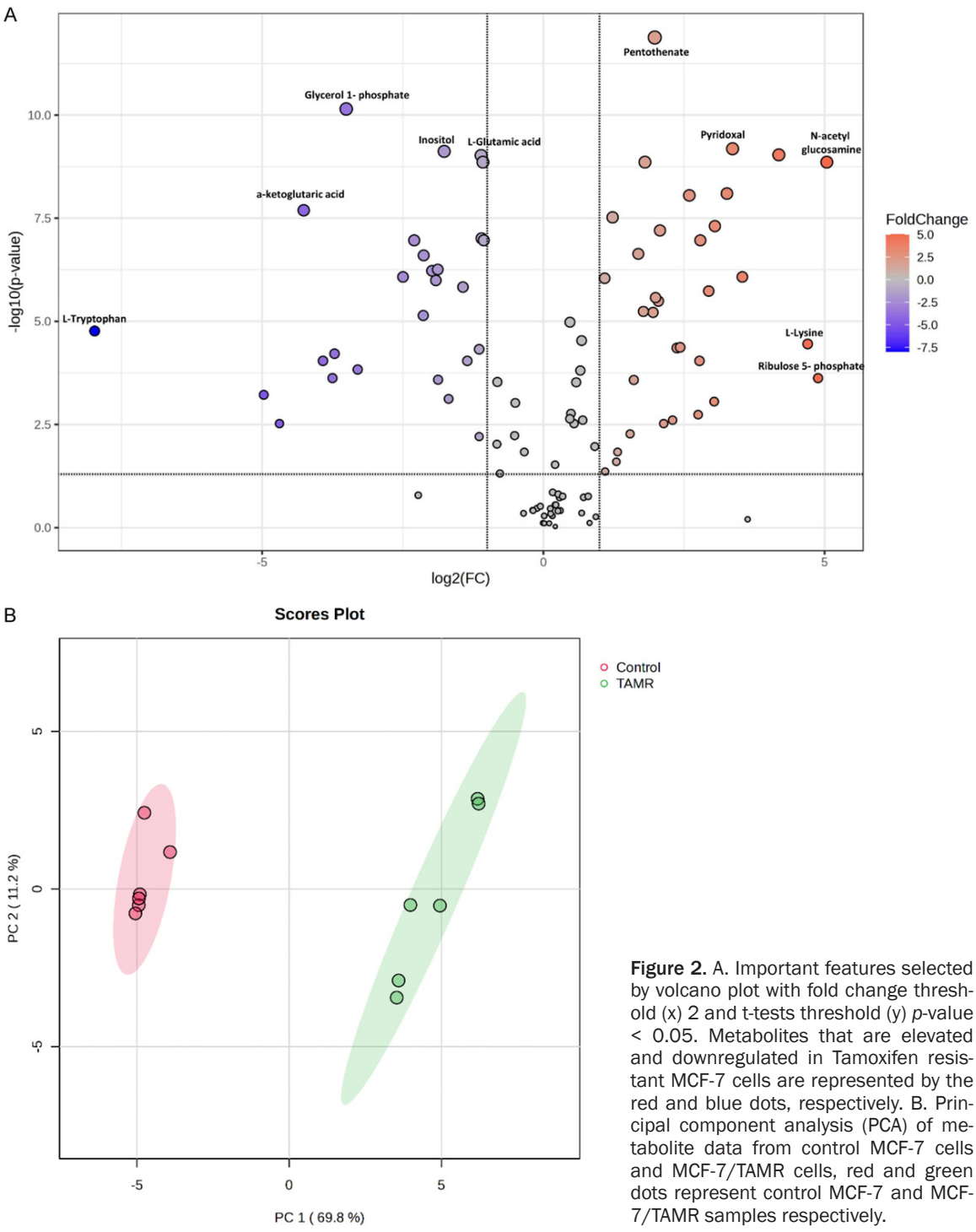

Figure 2. A. Important features selected by volcano plot with fold change threshold (x) 2 and t-tests threshold (y) *p*-value < 0.05. Metabolites that are elevated and downregulated in Tamoxifen resistant MCF-7 cells are represented by the red and blue dots, respectively. B. Principal component analysis (PCA) of metabolite data from control MCF-7 cells and MCF-7/TAMR cells, red and green dots represent control MCF-7 and MCF-7/TAMR samples respectively.

enriched pathways along with statistical analysis details.

Discussion

Both transcriptomic and metabolomics provide complimentary details regarding genetic modification, protein synthesis, metabolisms, and cellular function by reflecting changes in genotype and phenotype, respectively [29, 30]. The analysis of the metabolome of cancer cells has lately received interest as a diagnostic tool for the development and progression of cancer [31]. Metabolic reprogramming is thought to be

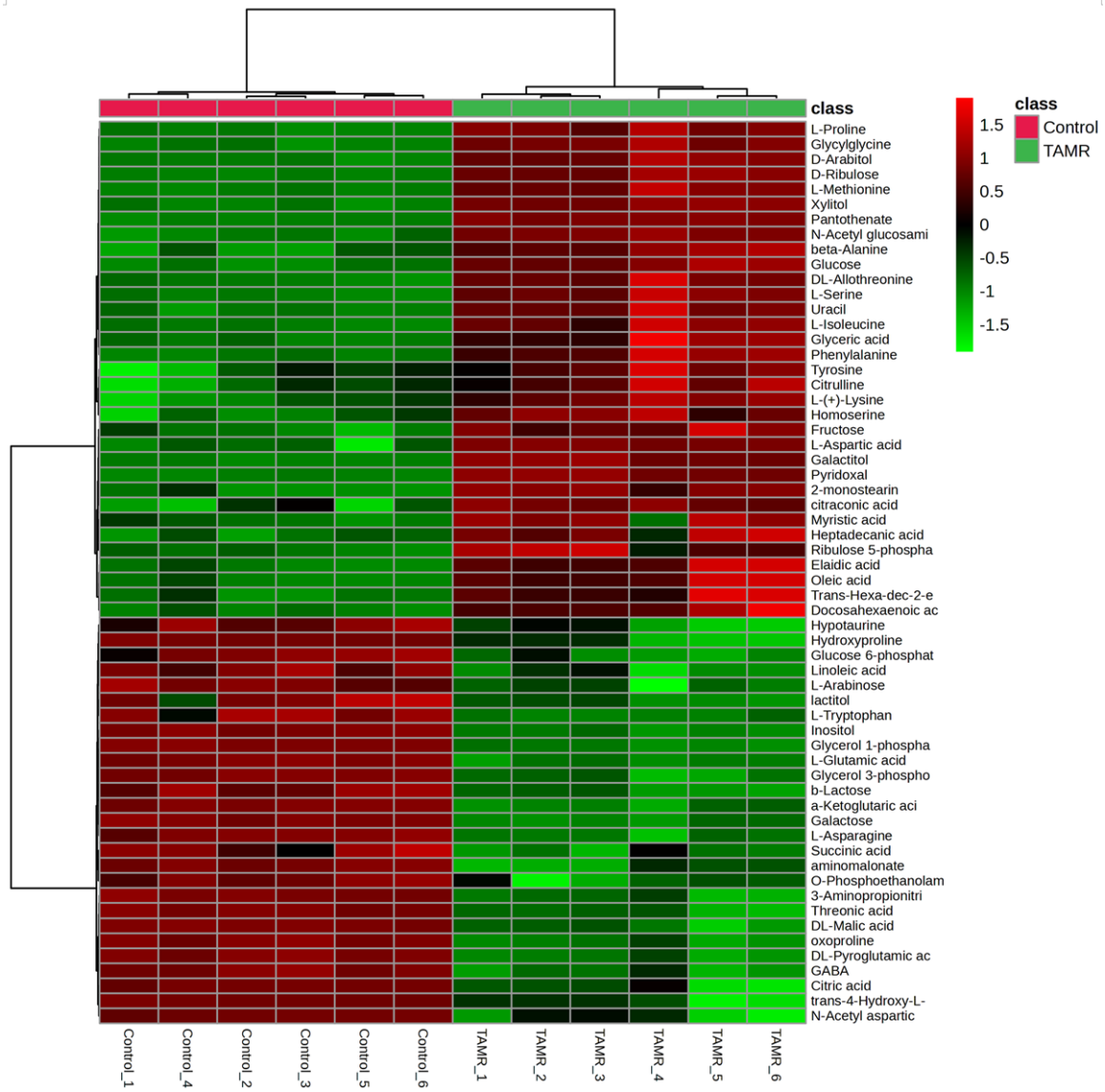

Figure 3. Heat Map. Clustering analysis of differentially expressed metabolites in MCF-7 cells and MCF-7/TAMR cells (distance measured using Euclidean, and clustering algorithm using ward D).

one of the characteristics of cancer [32]. In addition to influencing tumor development and patient survival, metabolic changes may play a role in mediating drug resistance [33, 34]. Metabolomics of chemo resistant cancer cells may reveal possible targets and inspire the creation of new therapeutic strategies for the treatment of the disease. In this study, we performed untargeted metabolomics analysis and found various deregulated metabolites in MCF-7/TAMR cells compared to parental MCF-7 cells. N-acetyl-D-glucosamine was the most significantly upregulated metabolite (fold change = 30, $P < 0.001$) in TAMR cells, which is an important metabolite of the hexosamine biosynthesis pathway (HBP). This suggests that in TAMR cells, the HBP pathway is upregulated. N-Acetyl-D-glucosamine is used for post-translational modification of the serine and threonine residues in proteins by the enzyme O-linked N-acetylgluocosmaine transferase (OGT). As previously reported, treatment-inducing O-GlcNAcylation protects breast cancer cells from TAM-induced cell death [35]. TAMR cells contain higher levels of pantothenic acid (fold change = 3.5, $P < 0.001$) and beta-alanine (fold change = 3.2005, $P < 0.001$). A study previously linked these metabolites to the glyco-

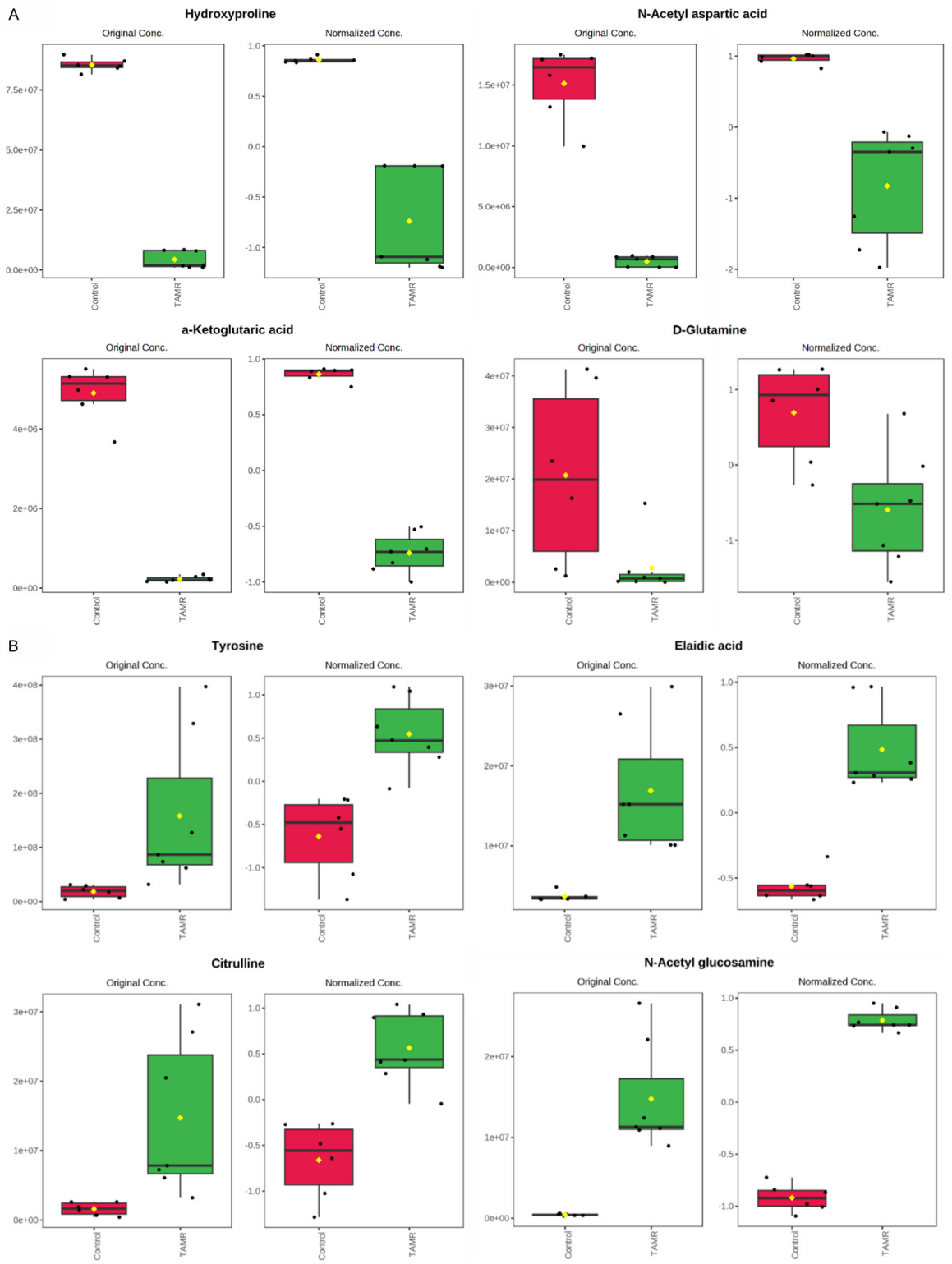

Figure 4. Box and Whisker plot representing significantly deregulated metabolites ($P < 0.05$) in MCF-7 (red) and MCF-7/TAMR (green) cells. The X axes depicts metabolite, while Y axes represents the metabolite's relative concentration. The box plots display interquartile ranges as boxes, with a horizontal line representing the median (50th percentile) within the box. The bottom and top of the boxes correspond to the 25th and 75th percentiles, respectively. The lower whisker represents the 5th percentile, while the higher whisker represents the 95th percentile. A. Downregulated metabolites in Tamoxifen resistant cells. B. Upregulated metabolites in Tamoxifen resistant cells.

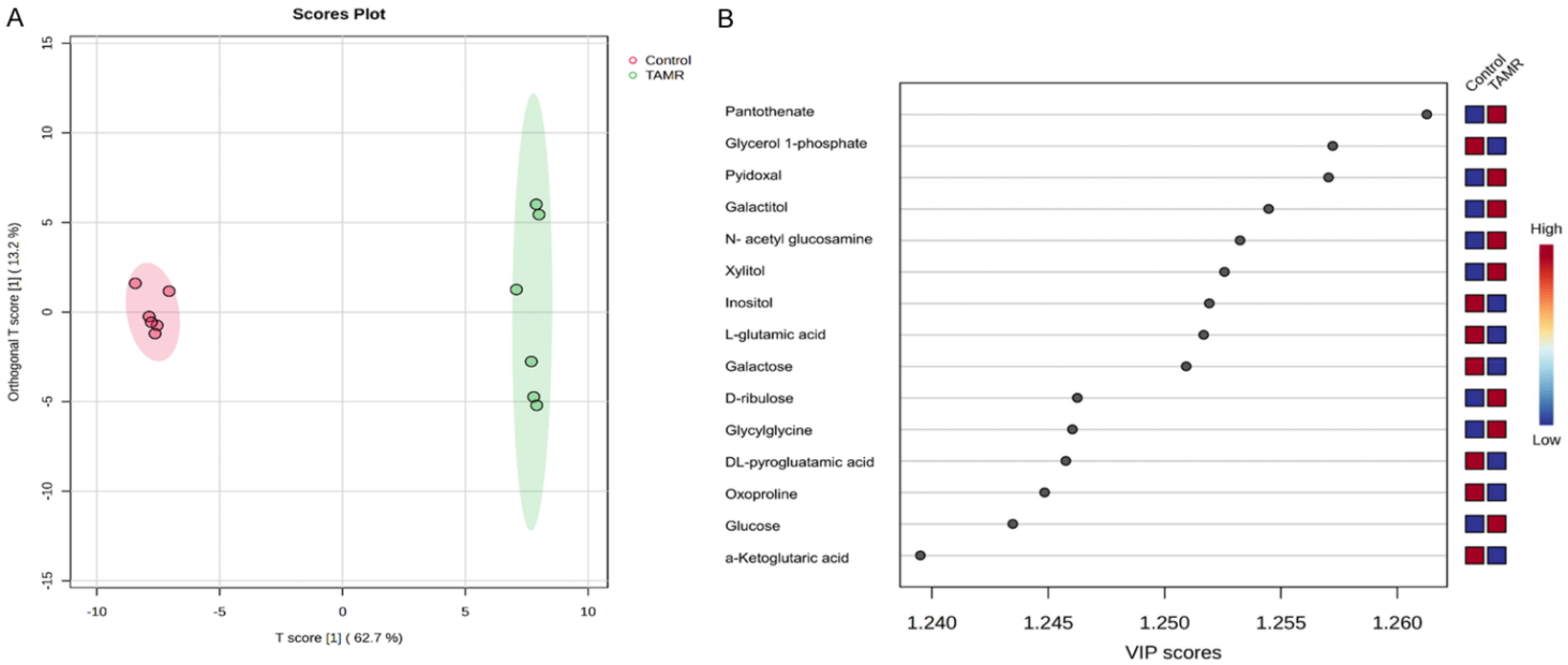

Figure 5. A. Two-dimensional representations of the Orthogonal Partial least square discriminant analysis (OPLS-DA) models to discriminate the Tamoxifen resistant (TAMR) cells and Control MCF-7 cells. B. The top 15 metabolites with Variable Importance in Projection score of 1.0 or above are displayed. The right-hand boxes show the relative concentration of the respective metabolite in each group being studied.

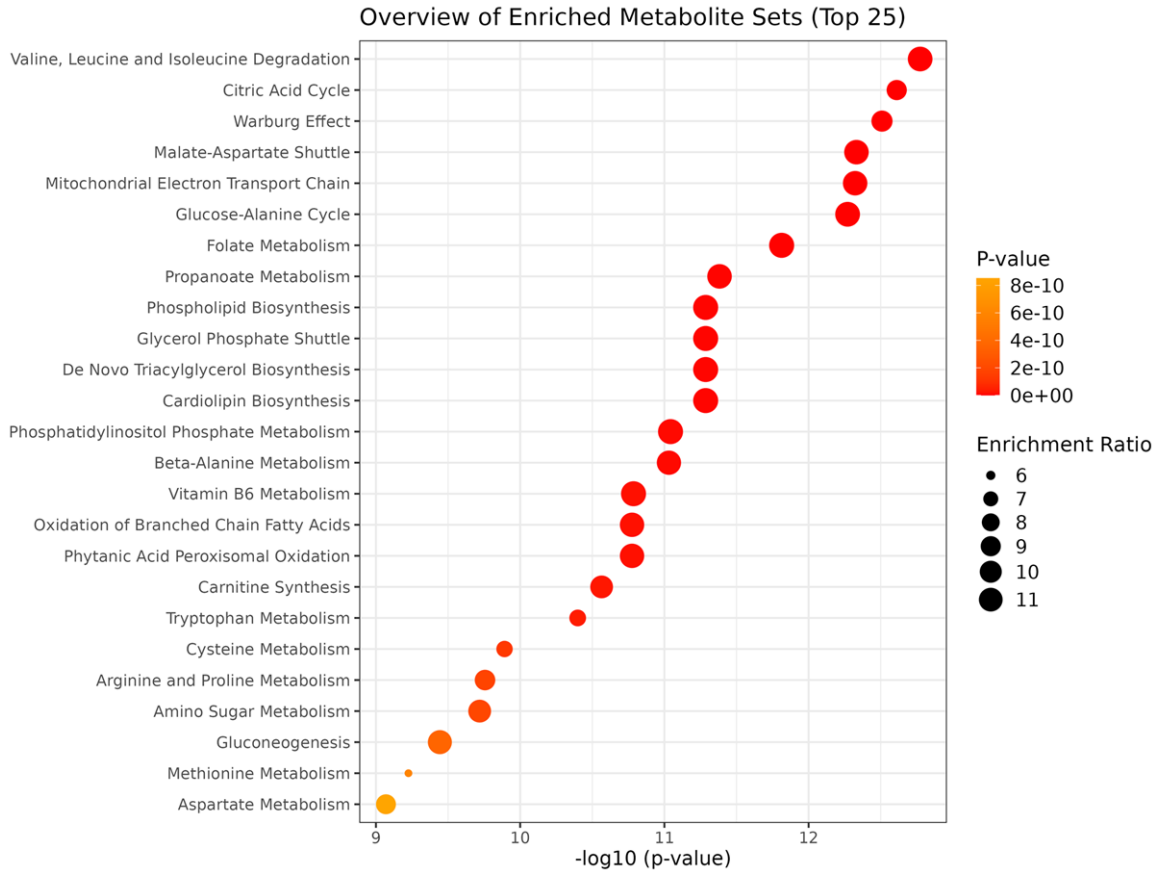

Figure 6. Dot Plot representing Quantitative enrichment analysis of deregulated metabolites in TAM resistance breast cancer cells by using global test.

lytic activity and tumor aggressiveness in breast cancer cells [36].

We identified various lipids that were significantly deregulated in TAMR, which include myo-inositol, docosahexaenoic acid, oleic acid, arachidonic acid, and palmitoleic acid. The TAMR cells displayed a notable reduction in myo-inositol, a part of membrane lipids. Myo-inositol has been reported to have many anti-cancer effects, including pro-apoptotic and anti-proliferative effects in different cancer types, and dysregulation of inositol metabolism has been linked to cancer [37]. We have detected an upregulation of the arachidonic acid level in TAMR cells. It has been shown that arachidonic acid can activate PI3K pathways in cancer [38], which are also found to be elevated in TMAR cells [39, 40]. Additionally, arachidonic acid metabolite has also been identified as a potential therapeutic target in breast cancer aggressiveness and metastasis [41]. Docosahexaenoic acid was significantly increased (fold change = 4.8245, $P < 0.001$) in the TAMR cell. It is one of the fatty acid ligands of free fatty acid receptor 4 (FFAR4) and activates extracellular-signal-regulated kinase (ERK) and AKT pathways to produce the TAMR phenotype [42].

Among the deregulated amino acids, tryptophan, an essential amino acid, was found to be downregulated in MCF-7/TAMR cells. Tryptophan catabolism has been found to be upregulated in breast cancer patients compared to healthy individuals [43, 44]. Tryptophan is converted to kynurenine by the enzyme Indoleamine 2,3-dioxygenase (IDO), and increased IDO expression is correlated to tumor aggressiveness, poor prognosis, and chemoresistance against paclitaxel in breast cancer [45]. This suggests the role of tryptophan degradation in TAMR breast cancer cells.

Serine and phosphoserine are found in higher concentrations in TAMR cells. Serine upregula-

Table 2. Statistical summary of enriched metabolic pathways in Tamoxifen resistant cells obtained by quantitative enrichment analysis

Enriched Pathway	Total Compound	Hits	Raw p	Holm p
Valine, Leucine and Isoleucine Degradation	60	5	1.69E-13	1.33E-11
Citric Acid Cycle	32	4	2.45E-13	1.91E-11
Warburg Effect	58	8	3.10E-13	2.39E-11
Malate-Aspartate Shuttle	10	4	4.66E-13	3.54E-11
Mitochondrial Electron Transport Chain	19	2	4.76E-13	3.57E-11
Glucose-Alanine Cycle	13	3	5.37E-13	3.97E-11
Folate Metabolism	29	1	1.54E-12	1.12E-10
Propanoate Metabolism	42	3	4.15E-12	2.99E-10
Phospholipid Biosynthesis	29	1	5.18E-12	3.68E-10
Glycerol Phosphate Shuttle	11	1	5.18E-12	3.68E-10
De Novo Triacylglycerol Biosynthesis	9	1	5.18E-12	3.68E-10
Cardiolipin Biosynthesis	11	1	5.18E-12	3.68E-10
Phosphatidylinositol Phosphate Metabolism	17	1	9.07E-12	6.08E-10
Beta-Alanine Metabolism	34	6	9.30E-12	6.14E-10
Vitamin B6 Metabolism	20	1	1.64E-11	1.06E-09
Oxidation of Branched Chain Fatty Acids	26	2	1.68E-11	1.07E-09
Phytanic Acid Peroxisomal Oxidation	26	2	1.68E-11	1.07E-09
Carnitine Synthesis	22	4	2.73E-11	1.69E-09
Tryptophan Metabolism	60	3	3.99E-11	2.44E-09
Cysteine Metabolism	26	3	1.28E-10	7.70E-09
Arginine and Proline Metabolism	53	8	1.75E-10	1.03E-08
Amino Sugar Metabolism	33	4	1.91E-10	1.11E-08
Gluconeogenesis	35	4	3.60E-10	2.05E-08
Methionine Metabolism	43	6	5.95E-10	3.33E-08

tion indicates an increase in the serine biosynthetic pathway, which has been linked to many cancers [46, 47]. Phosphoserine is formed in the serine biosynthetic pathway by the enzyme PSAT1, which converts 3-phospho-hydroxypyruvate into phosphoserine. A study reported upregulation of the PSAT1 enzyme in patients receiving adjuvant TAM [48]. This suggests a critical role of these metabolites in TAMR resistance.

In TAMR cells, the amount of pyroglutamic acid showed a significant decrease. The reduction might reflect a decrease in the amounts of glutamine and/or glutamic acid. This is because glutamine and glutamic acid are known to undergo cyclization to form pyroglutamic acid in the ionization source [49]. Consequently, the significant decrease in pyroglutamic acid may function as a possible biomarker for TAMR.

Sugar alcohols, namely galactitol, arabitol, and xylitol were discovered to be the most significant ($P < 0.05$) deregulated metabolites that differentiated TAMR cells from control MCF-7 cells. According to the findings of a study, the concentration of sugar alcohol was significantly higher in hepatocellular carcinoma than in normal liver tissue [50]. The concentration of sugar alcohol can differentiate between malignant and nonmalignant cancer.

Among the enriched pathways, TCA cycle was found to be decreased in TAMR cells. It has been shown that TAMR cells have lower levels of citric acid, succinic acid, and oxoglutaric acid, which are all byproducts of the TCA cycle. This clearly indicates that the TCA cycle is suppressed in TAMR cells. To compensate energy required for growing TAMR cells, they activate the Warburg effect.

Furthermore, we have identified an enriched pathway, the malate-aspartate shuttle (Borst cycle), which is known to support cellular metabolic fitness by producing NADH and assisting

cancer cells to withstand drug effects [51]. The discriminatory metabolites associated with this pathway are Aspartate (fold change = 3.7515, P < 0.001), malate (fold change = 0.24738, P < 0.001), glutamic acid, and oxoglutaric acid. Another significantly enriched pathway identified is propanoate metabolism. The deregulated metabolites associated with this pathway are beta-alanine, L-glutamic acid, and oxoglutaric acid. Deregulated propanoate metabolism has been linked to breast cancer metastasis and aggressiveness [52], indicating its importance in TAMR breast cancer.

Conclusion

This study is the first to use GC-MS-based metabolomics to demonstrate that TAMR breast cancer switches its metabolism to sustain its growth and proliferation and develop acquired resistance. In conclusion, we have identified metabolites, namely glycerol 1-phosphate, pyridoxal, inositol, galactitol, xylitol, n-acetyl-d-glucosamine, pantothenate, pyroglutamic acid, L-glutamic acid, glycyl-glycine, galactose, and D-ribulose, that significantly differentiate between control MCF-7 and MCF-7/TAMR cells based on their VIP score. Furthermore, we discovered top-enriched pathways of deregulated metabolites such as valine, leucine, and isoleucine degradation, citric acid cycle, Warburg effect, malate-aspartate shuttle, mitochondrial electron transport chain, glucose-alanine cycle, folate metabolism, and propanoate metabolism. Many of these pathways have been linked to aggressiveness, metastasis, and drug resistance in breast and other cancers. Altered metabolite levels and metabolic pathways can potentially indicate future therapeutic strategies in the acquired anti-cancer drug resistance in recalcitrant breast cancer.

Disclosure of conflict of interest

None.

Address correspondence to: Dr. Ashutosh Shrivastava, Center for Advance Research, Faculty of Medicine, King George's Medical University, Lucknow, Uttar Pradesh 226003, India. E-mail: ashutoshshrivastava@kgmcindia.edu

References

[1] World Cancer Report: Cancer Research for Cancer Prevention. IARC Publications; 2020.

[2] Loibl S, Poortmans P, Morrow M, Denkert C and Curigliano G. Breast cancer. Lancet 2021; 397: 1750-1769.

[3] Zhang MH, Man HT, Zhao XD, Dong N and Ma SL. Estrogen receptor-positive breast cancer molecular signatures and therapeutic potentials (Review). Biomed Rep 2014; 2: 41-52.

[4] Cole MP, Jones CT and Todd ID. A new anti-oestrogenic agent in late breast cancer. An early clinical appraisal of ICI46474. Br J Cancer 1971; 25: 270-275.

[5] Fisher B, Costantino JP, Wickerham DL, Redmond CK, Kavanah M, Cronin WM, Vogel V, Robidoux A, Dimitrov N, Atkins J, Daly M, Wieand S, Tan-Chiu E, Ford L and Wolmark N. Tamoxifen for prevention of breast cancer: report of the national surgical adjuvant breast and bowel project P-1 study. J Natl Cancer Inst 1998; 90: 1371-1388.

[6] Ring A and Dowsett M. Mechanisms of tamoxifen resistance. Endocr Relat Cancer 2004; 11: 643-658.

[7] Fan W, Chang J and Fu P. Endocrine therapy resistance in breast cancer: current status, possible mechanisms and overcoming strategies. Future Med Chem 2015; 7: 1511-1519.

[8] Yao J, Deng K, Huang J, Zeng R and Zuo J. Progress in the understanding of the mechanism of tamoxifen resistance in breast cancer. Front Pharmacol 2020; 11: 592912.

[9] Viedma-Rodríguez R, Baiza-Gutman L, Salamanca-Gómez F, Diaz-Zaragoza M, Martínez-Hernández G, Ruiz Esparza-Garrido R, Velázquez-Flores MA and Arenas-Aranda D. Mechanisms associated with resistance to tamoxifen in estrogen receptor-positive breast cancer (Review). Oncol Rep 2014; 32: 3-15.

[10] Faubert B, Solmonson A and DeBerardinis RJ. Metabolic reprogramming and cancer progression. Science 2020; 368: eaaw5473.

[11] Pranzini E, Pardella E, Paoli P, Fendt SM and Taddei ML. Metabolic reprogramming in anticancer drug resistance: a focus on amino acids. Trends Cancer 2021; 7: 682-699.

[12] DeBerardinis RJ and Chandel NS. Fundamentals of cancer metabolism. Sci Adv 2016; 2: e1600200.

[13] Zhang A, Sun H, Xu H, Qiu S and Wang X. Cell metabolomics. OMICS 2013; 17: 495-501.

[14] Dettmer K, Aronov PA and Hammock BD. Mass spectrometry-based metabolomics. Mass Spectrom Rev 2007; 26: 51-78.

[15] Sharaf BM, Giddey AD, Alniss H, Al-Hroub HM, El-Awady R, Mousa M, Almehdi A, Soares NC and Semreen MH. Untargeted metabolomics of breast cancer cells MCF-7 and SkBr3 treated with tamoxifen/trastuzumab. Cancer Genomics Proteomics 2022; 19: 79-93.

[16] Semreen MH, Alniss H, Cacciatore S, El-Awady R, Mousa M, Almehdi AM, El-Huneidi W, Zerbini

L and Soares NC. GC-MS based comparative metabolomic analysis of MCF-7 and MDA-MB-231 cancer cells treated with Tamoxifen and/or Paclitaxel. J Proteomics 2020; 225: 103875.
[17] Kim HS, Tian L, Kim H and Moon WK. Investigation of discriminant metabolites in tamoxifen-resistant and choline kinase-alpha-down-regulated breast cancer cells using 1H-nuclear magnetic resonance spectroscopy. PLoS One 2017; 12: e0179773.
[18] Comşa Ş, Cîmpean AM and Raica M. The story of MCF-7 breast cancer cell line: 40 years of experience in research. Anticancer Res 2015; 35: 3147-3154.
[19] He Y, Zhang ZM, Ma P, Ji HC and Lu HM. GC-MS profiling of leukemia cells: an optimized preparation protocol for the intracellular metabolome. Anal Methods 2018; 10: 1266-1274.
[20] Sellick CA, Hansen R, Stephens GM, Goodacre R and Dickson AJ. Metabolite extraction from suspension-cultured mammalian cells for global metabolite profiling. Nat Protoc 2011; 6: 1241-1249.
[21] Srivastava A, Mishra A and Shrivastava A. Optimizing solvents and derivatizing agents for metabolomic profiling of human plasma using GC-MS. Chromatographia 2023; 86: 523-534.
[22] Tsugawa H, Cajka T, Kind T, Ma Y, Higgins B, Ikeda K, Kanazawa M, VanderGheynst J, Fiehn O and Arita M. MS-DIAL: data-independent MS/MS deconvolution for comprehensive metabolome analysis. Nat Methods 2015; 12: 523-526.
[23] Horai H, Arita M, Kanaya S, Nihei Y, Ikeda T, Suwa K, Ojima Y, Tanaka K, Tanaka S, Aoshima K, Oda Y, Kakazu Y, Kusano M, Tohge T, Matsuda F, Sawada Y, Hirai MY, Nakanishi H, Ikeda K, Akimoto N, Maoka T, Takahashi H, Ara T, Sakurai N, Suzuki H, Shibata D, Neumann S, Iida T, Tanaka K, Funatsu K, Matsuura F, Soga T, Taguchi R, Saito K and Nishioka T. MassBank: a public repository for sharing mass spectral data for life sciences. J Mass Spectrom 2010; 45: 703-714.
[24] Pang Z, Chong J, Zhou G, de Lima Morais DA, Chang L, Barrette M, Gauthier C, Jacques PÉ, Li S and Xia J. MetaboAnalyst 5.0: narrowing the gap between raw spectra and functional insights. Nucleic Acids Res 2021; 49: W388-W396.
[25] Hutschenreuther A, Kiontke A, Birkenmeier G and Birkemeyer C. Comparison of extraction conditions and normalization approaches for cellular metabolomics of adherent growing cells with GC-MS. Anal Methods 2012; 4: 1953-1963.
[26] Goeman JJ, van de Geer SA, de Kort F and van Houwelingen HC. A global test for groups of genes: testing association with a clinical outcome. Bioinformatics 2004; 20: 93-99.
[27] Kanehisa M and Goto S. KEGG: Kyoto encyclopedia of genes and genomes. Nucleic Acids Res 2000; 28: 27-30.
[28] Jewison T, Su Y, Disfany FM, Liang Y, Knox C, Maciejewski A, Poelzer J, Huynh J, Zhou Y, Arndt D, Djoumbou Y, Liu Y, Deng L, Guo AC, Han B, Pon A, Wilson M, Rafatnia S, Liu P and Wishart DS. SMPDB 2.0: big improvements to the Small Molecule Pathway Database. Nucleic Acids Res 2014; 42: D478-484.
[29] Liu JL, Zhang WQ, Zhao M and Huang MY. Integration of transcriptomic and metabolomic data reveals enhanced steroid hormone biosynthesis in mouse uterus during decidualization. Proteomics 2017; 17.
[30] Zhang G, He P, Tan H, Budhu A, Gaedcke J, Ghadimi BM, Ried T, Yfantis HG, Lee DH, Maitra A, Hanna N, Alexander HR and Hussain SP. Integration of metabolomics and transcriptomics revealed a fatty acid network exerting growth inhibitory effects in human pancreatic cancer. Clin Cancer Res 2013; 19: 4983-4993.
[31] Schmidt DR, Patel R, Kirsch DG, Lewis CA, Vander Heiden MG and Locasale JW. Metabolomics in cancer research and emerging applications in clinical oncology. CA Cancer J Clin 2021; 71: 333-358.
[32] Pavlova NN and Thompson CB. The emerging hallmarks of cancer metabolism. Cell Metab 2016; 23: 27-47.
[33] Desbats MA, Giacomini I, Prayer-Galetti T and Montopoli M. Metabolic plasticity in chemotherapy resistance. Front Oncol 2020; 10: 281.
[34] Mishra A, Srivastava A, Pateriya A, Tomar MS, Mishra AK and Shrivastava A. Metabolic reprograming confers tamoxifen resistance in breast cancer. Chem Biol Interact 2021; 347: 109602.
[35] Kanwal S, Fardini Y, Pagesy P, N'Tumba-Byn T, Pierre-Eugène C, Masson E, Hampe C and Issad T. O-GlcNAcylation-inducing treatments inhibit estrogen receptor α expression and confer resistance to 4-OH-tamoxifen in human breast cancer-derived MCF-7 cells. PLoS One 2013; 8: e69150.
[36] Hutschenreuther A, Birkenmeier G, Bigl M, Krohn K and Birkemeyer C. Glycerophosphoglycerol, beta-alanine, and pantothenic acid as metabolic companions of glycolytic activity and cell migration in breast cancer cell lines. Metabolites 2013; 3: 1084-1101.
[37] Tan J, Yu CY, Wang ZH, Chen HY, Guan J, Chen YX and Fang JY. Genetic variants in the inositol phosphate metabolism pathway and risk of different types of cancer. Sci Rep 2015; 5: 8473.

[38] Hughes-Fulford M, Li CF, Boonyaratanakornkit J and Sayyah S. Arachidonic acid activates phosphatidylinositol 3-kinase signaling and induces gene expression in prostate cancer. Cancer Res 2006; 66: 1427-1433.
[39] Hamadneh L, Abuarqoub R, Alhusban A and Bahader M. Upregulation of PI3K/AKT/PTEN pathway is correlated with glucose and glutamine metabolic dysfunction during tamoxifen resistance development in MCF-7 cells. Sci Rep 2020; 10: 21933.
[40] Dong C, Wu J, Chen Y, Nie J and Chen C. Activation of PI3K/AKT/mTOR pathway causes drug resistance in breast cancer. Front Pharmacol 2021; 12: 628690.
[41] Borin TF, Angara K, Rashid MH, Achyut BR and Arbab AS. Arachidonic acid metabolite as a novel therapeutic target in breast cancer metastasis. Int J Mol Sci 2017; 18: 2661.
[42] Chu X, Zhou Q, Xu Y, Jiang J, Li Q, Zhou Q, Wu Q, Jin M, Wang H, Gu Y, Wang X, Wang B, He S, He X, Wu C, Zhang F and Zhang Y. Aberrant fatty acid profile and FFAR4 signaling confer endocrine resistance in breast cancer. J Exp Clin Cancer Res 2019; 38: 100.
[43] Onesti CE, Boemer F, Josse C, Leduc S, Bours V and Jerusalem G. Tryptophan catabolism increases in breast cancer patients compared to healthy controls without affecting the cancer outcome or response to chemotherapy. J Transl Med 2019; 17: 239.
[44] Juhász C, Nahleh Z, Zitron I, Chugani DC, Janabi MZ, Bandyopadhyay S, Ali-Fehmi R, Mangner TJ, Chakraborty PK, Mittal S and Muzik O. Tryptophan metabolism in breast cancers: molecular imaging and immunohistochemistry studies. Nucl Med Biol 2012; 39: 926-932.
[45] Zhao Y, Wei L, Liu J and Li F. Chemoresistance was correlated with elevated expression and activity of indoleamine 2,3-dioxygenase in breast cancer. Cancer Chemother Pharmacol 2020; 85: 77-93.
[46] Mattaini KR, Sullivan MR and Vander Heiden MG. The importance of serine metabolism in cancer. J Cell Biol 2016; 214: 249-257.
[47] Sullivan MR, Mattaini KR, Dennstedt EA, Nguyen AA, Sivanand S, Reilly MF, Meeth K, Muir A, Darnell AM, Bosenberg MW, Lewis CA and Vander Heiden MG. Increased serine synthesis provides an advantage for tumors arising in tissues where serine levels are limiting. Cell Metab 2019; 29: 1410-1421, e1414.
[48] De Marchi T, Timmermans MA, Sieuwerts AM, Smid M, Look MP, Grebenchtchikov N, Sweep FCGJ, Smits JG, Magdolen V, van Deurzen CHM, Foekens JA, Umar A and Martens JW. Phosphoserine aminotransferase 1 is associated to poor outcome on tamoxifen therapy in recurrent breast cancer. Sci Rep 2017; 7: 2099.
[49] Purwaha P, Silva LP, Hawke DH, Weinstein JN and Lorenzi PL. An artifact in LC-MS/MS measurement of glutamine and glutamic acid: in-source cyclization to pyroglutamic acid. Anal Chem 2014; 86: 5633-5637.
[50] Ismail IT, Fiehn O, Elfert A, Helal M, Salama I and El-Said H. Sugar alcohols have a key role in pathogenesis of chronic liver disease and hepatocellular carcinoma in whole blood and liver tissues. Cancers (Basel) 2020; 12: 484.
[51] Muthu M, Kumar R, Syed Khaja AS, Gilthorpe JD, Persson JL and Nordström A. GLUL ablation can confer drug resistance to cancer cells via a malate-aspartate shuttle-mediated mechanism. Cancers (Basel) 2019; 11: 1945.
[52] Schramm G, Surmann EM, Wiesberg S, Oswald M, Reinelt G, Eils R and Konig R. Analyzing the regulation of metabolic pathways in human breast cancer. BMC Med Genomics 2010; 3: 39.

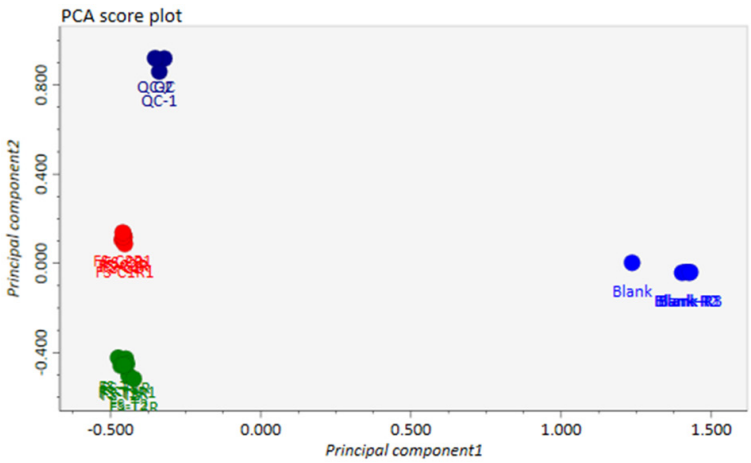

Supplementary Figure 1. Principal Component Analysis (PCA) plot demonstrates the clustering patterns seen among quality control (QC) samples.